Journal of Vertebrate Paleontology

ISSN: 0272-4634 (Print) 1937-2809 (Online) Journal homepage: http://www.tandfonline.com/loi/ujvp20

A new fossil species of *Boa* Linnaeus, 1758 (Squamata, Boidae), from the Pleistocene of Marie-Galante Island (French West Indies)

Corentin Bochaton & Salvador Bailon

To cite this article: Corentin Bochaton & Salvador Bailon (2018) A new fossil species of *Boa* Linnaeus, 1758 (Squamata, Boidae), from the Pleistocene of Marie-Galante Island (French West Indies), Journal of Vertebrate Paleontology, 38:3, e1462829, DOI: 10.1080/02724634.2018.1462829

To link to this article: https://doi.org/10.1080/02724634.2018.1462829

Journal of Vertebrate Paleontology e1462829 (14 pages)
Published with license by the Society of Vertebrate Paleontology
DOI: 10.1080/02724634.2018.1462829

ARTICLE

A NEW FOSSIL SPECIES OF *BOA* LINNAEUS, 1758 (SQUAMATA, BOIDAE), FROM THE PLEISTOCENE OF MARIE-GALANTE ISLAND (FRENCH WEST INDIES)

CORENTIN BOCHATON, *[,1,2,3] and SALVADOR BAILON[2,4]
[1]Max Planck Institute for the Science of Human History, 10 Kahlaische Strasse, 07745 Jena, Germany, bochaton@shh.mpg.de;
[2]Laboratoire 'Archéozoologie et Archéobotanique: Sociétés, Pratiques et Environnements,' UMR 7209, CNRS, MNHN, Muséum national d'Histoire naturelle, Sorbonne Universités, 55 rue Buffon, CP 56, 75005 Paris, France;
[3]Institut de Systématique, Évolution, Biodiversité, UMR 7205, CNRS, MNHN, UPMC, EPHE, Muséum national d'Histoire naturelle, Sorbonne Universités, 57 rue Cuvier, CP 30, 75005 Paris, France;
[4]Laboratoire 'Histoire naturelle de l'Homme préhistorique,' UMR 7194, CNRS, UPVD, MNHN, Muséum national d'Histoire naturelle, Sorbonne Universités, 75013 Paris, France, salvador.bailon@mnhn.fr

ABSTRACT—Several studies have reported the occurrence of fossil remains of a now extinct *Boa* snake from the upper Pleistocene of Marie-Galante Island, French West Indies. However, these remains have never been fully investigated and no complete description of this possible new species has been published. In this paper, we try to bridge this gap by providing a detailed morphological study of the *Boa* remains discovered in the three major fossil deposits of Marie-Galante Island. Our study reveals the specific morphological aspects of this fossil snake and allows us to identify it as a new species, *Boa blanchardensis*. We also reconstructed its body size, carried out a paleohistological investigation, and suggest that this snake may have been a dwarf species. We then discuss the possible explanation for the extinction of this snake on Marie-Galante Island and possibly also on other Guadeloupe islands.

http://zoobank.org/urn:lsid:zoobank.org:pub:7E352396-4945-447D-80A8-C2D9057B39EB

SUPPLEMENTAL DATA—Supplemental materials are available for this article for free at www.tandfonline.com/UJVP

Citation for this article: Bochaton, C., and S. Bailon. 2018. A new fossil species of *Boa* Linnaeus, 1758 (Squamata, Boidae), from the Pleistocene of Marie-Galante Island (French West Indies). Journal of Vertebrate Paleontology. DOI: 10.1080/02724634.2018.1462829.

INTRODUCTION

The West Indies is considered one of the world's biodiversity hot spots on account of its rich, endemic fauna. This area is also known for its eventful history of human colonization, which is responsible for several extinctions during the past centuries (Brace et al., 2015; Kemp and Hadly, 2015; Soto-Centeno and Steadman, 2015; Steadman et al., 2015). On account of these phenomena, investigating the history of many regional taxa is a complex task. The Lesser Antilles is particularly subject to such difficulties because each terrestrial taxon occurring here is often represented by a single endemic species on each island. Due to this characteristic, and as a consequence of extinction events, several taxa display a discontinuous distribution across the Lesser Antillean islands. In the most extreme case, some taxa can even be relictual, with a single surviving species in the island chain, as is the case of the anguid lizard genus, *Diploglossus* Wiegmann, 1834, which currently only occurs on Montserrat Island (Underwood, 1964; Bochaton et al., 2015a), although fossil evidence of its past occurrence on other islands has recently started to emerge (Bochaton et al., 2016a). Another example of this is the large boid snake genus, *Boa* Linnaeus, 1758, which also shows a discontinuous distribution in the Lesser Antilles. Indeed, these snakes currently only occur on the islands of Saint Lucia and Dominica, where they are represented by two endemic species, *Boa orophias* Linnaeus, 1758, and *Boa nebulosa* Lazell, 1964, respectively (Powell and Henderson, 2012). However, considering the South American origin of the *Boa* genus (Albino, 2011; Head et al., 2012), and the central position of the two above-mentioned islands in the Lesser Antillean island chain, it is likely that *Boa* snakes occurred in the past on all the islands separating the northernmost islands of Dominica from continental South America. This hypothesis is partly confirmed by historical evidence demonstrating the past occurrence of *Boa* snakes on the islands of Martinique (Labat, 1724; Breuil, 2009) and Saint Vincent (Moreau de Jonnès, 1816), showing that these large snakes probably became extinct recently: during the 18th century on Martinique and during the 19th or 20th centuries on Saint Vincent. In addition, fossil evidence suggests the past occurrence of *Boa* snakes north of Dominica, as far as the northernmost island of Antigua, during the Holocene (Steadman et al., 1984; Pregill et al., 1988), but also on Marie-Galante Island during the Pleistocene (Stouvenot et al., 2014; Bailon et al., 2015; Bochaton et al., 2015b). This fossil evidence indicates that *Boa* may also have been present on all the Lesser Antillean islands separating Dominica from Antigua,

*Corresponding author.

Color versions of one or more of the figures in the article can be found online at www.tandfonline.com/ujvp.

Published online 29 May 2018

including the Guadeloupe islands. However, *Boa* fossil remains are absent from the latter archipelago, apart from Marie-Galante Island. In addition, although all available evidence of past occurrences of *Boa* in the Lesser Antilles dates from the late Holocene period, the fossil *Boa* of Marie-Galante Island seems to have become extinct at the end of the Pleistocene. This isolated extinction event remains difficult to explain, partly because the remains of this fossil snake have never undergone a detailed paleontological study. In addition, the case of the Marie-Galante *Boa* raises the possibility of a Pleistocene extinction of this genus in the Guadeloupe Archipelago, where it was never reported in historical texts (Du Tertre, 1654; Rochefort, 1658) or the archeological record (Pregill et al., 1994; Grouard, 2001, 2010; de Waal, 2006; Boudadi-Maligne et al., 2016), although its past occurrence in Guadeloupe is considered likely.

The aim of the present study is to enhance our knowledge of the sole known fossil *Boa* snake from the Guadeloupe islands, the fossil *Boa* of Marie-Galante Island. We provide new data concerning the morphology, taxonomic status, and biology of this snake, in order to discuss in a more accurate way the potential reasons for the extinction of *Boa* on Marie-Galante and possibly in the whole Guadeloupe archipelago. In order to do so, we performed a detailed morphological analysis of newly discovered and previously reported remains, along with a morphometric and paleohistological analysis of the vertebrae.

Institutional Abbreviations—**MCZ**, Museum of Comparative Zoology, Harvard University, Cambridge, Massachusetts, U.S.A.; **MEC**, Musée Edgard Clerc, Moule, Guadeloupe; **MNHN-UMR7209**, UMR 7209 laboratory collections of the Muséum national d'Histoire naturelle, Paris, France; **MNHN-ZA-AC**, comparative anatomy collections of the Muséum national d'Histoire naturelle, Paris, France.

MATERIALS AND METHODS

Fossil and Comparative Samples

The studied fossil material includes 297 boid snake remains collected from Cadet 2 cave (16 specimens) (Bochaton et al., 2015b), Cadet 3 rock shelter (four specimens) (Sierpe, 2011; Stouvenot et al., 2014), and Blanchard Cave (277 specimens) (Bailon et al., 2015; Stoetzel et al., 2016) on Marie-Galante Island (Fig. 1). *Boa* remains were only found in the oldest layers of these three deposits, all dating from the late Pleistocene, and were absent from the subsequent Holocene layers (Stouvenot et al., 2014; Bailon et al., 2015; Bochaton et al., 2015b). Details concerning the stratigraphy of the deposits, taphonomy of the assemblages, and stratigraphic positions of the investigated boid remains can be found in the previously published studies of Cadet 2 cave (Bochaton et al., 2015b), Cadet 3 rock shelter (Stouvenot et al., 2014), and Blanchard Cave (Bailon et al., 2015). Marie-Galante boid remains were studied as part of a broad review of the squamate remains contained in the numerous archeological and paleontological deposits situated on all Guadeloupe islands (see a list of studied deposits in Bochaton et al., 2016b). With the exception of the three Marie-Galante sites mentioned above, all Guadeloupe deposits appeared to be free of boid remains, with the exception of a single archaeological artifact, a worked vertebra possibly transported from another island collected in the archeological site of Cathédrale de Basse-Terre (C.B., pers. observ.). The fossil material described in this study is stored at the MEC.

The comparative material used in this study comes from the MNHN-ZA-AC and the UMR 7209, the MEC, and the MCZ. They correspond to four specimens of *Boa nebulosa* (MNHN-ZA-AC 2016-1, MNHN-ZA-AC 2016-2, MEC-Boa 3, and MCZ 60802), four specimens of continental *Boa constrictor* from South America (MNHN-ZA-AC 1876-250, MNHN-ZA-AC 1876-618, MNHN-UMR7209-335, and MNHN-UMR7209-672), and four specimens of *Boa constrictor* of unknown provenance exhibiting a similar skeletal morphology to the other observed *B. constrictor* specimens (MNHN-ZA-AC 1884–2444, MNHN-ZA-AC 1890-115, MNHN-ZA-AC 1905-4, and MCZ 172037).

Systematic and Anatomical Nomenclature

Following Henderson and Powell (2009), we consider the *Boa* occurring in the different Lesser Antillean islands as a species rather than subspecies of *Boa constrictor*. The taxonomy of *Boa* is still subject to much discussion (Graham Reynolds et al., 2014; Card et al., 2016), but, to our knowledge, the Lesser Antillean

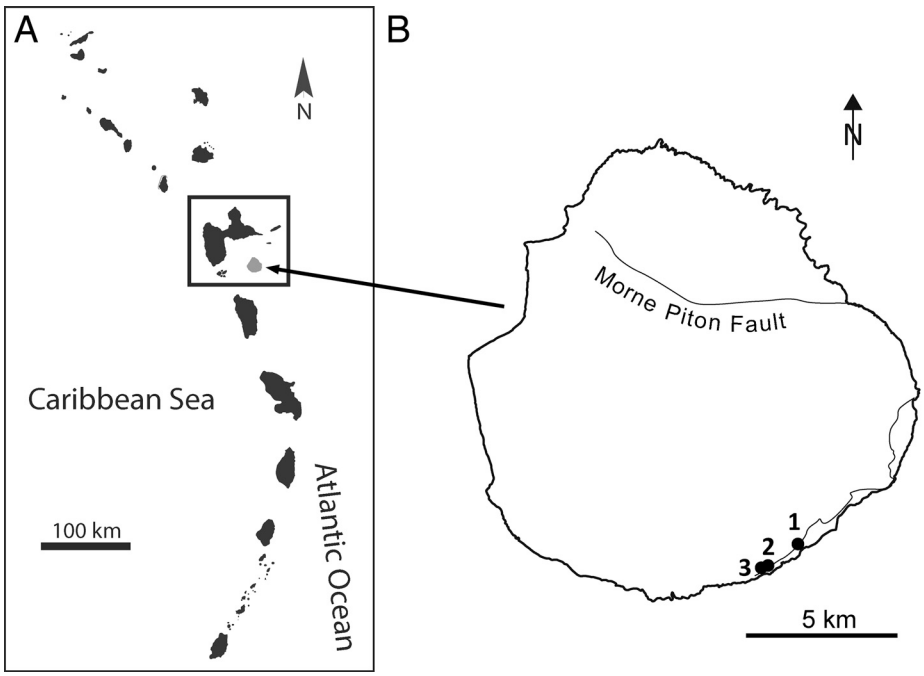

FIGURE 1. **A**, map of the Lesser Antilles indicating the position of the Guadeloupe Archipelago and Marie-Galante Island. **B**, map of Marie-Galante Island with the three deposits that preserve boid remains. **1**, Blanchard Cave; **2**, Cadet 2 cave; **3**, Cadet 3 rock shelter.

species have never been included in any molecular phylogenetic analysis. Due to the lack of information concerning our comparative sample of mainland South American *Boa*, they are all considered as *Boa constrictor*, the species name still used for the South American representatives of the genus.

The anatomical nomenclature used mostly follows Cundall and Irish (2008) for the skull. The terms used to describe the braincase follow Hoffstetter (1939) and Rieppel (1979). The nomenclature for the ribs and the vertebrae follows Hoffstetter and Gasc (1969), and Szyndlar (1984). For convenience, we use the term 'cervical' vertebrae informally for the anterior-most trunk vertebrae bearing a hypapophysis ('precloacal anterior vertebrae' sensu Albino, 2011).

Paleohistological Investigation

In order to perform histological observations on fossil vertebrae, three vertebrae were embedded in polyester resin, sectioned along their transverse axis, mounted on a glass slide, and then polished to obtain 100 μm thick ground sections. The slides were then observed with a compound microscope in natural and polarized light. These three vertebrae were selected among the largest collected fossil elements in order to identify the oldest possible specimens at the time of their death; they were all collected in the Pleistocene 'layer 8' of Blanchard Cave deposit.

Morphometric Analysis

Morphometric data include six measurements taken on trunk vertebrae using a dial caliper (Mitutoyo IP 67) by a single user (C.B.). Most of these measurements (Fig. 2) are from Szyndlar (1984), Rage (2001), and Albino (2011) and are widely used for snake vertebrae. Subsequent statistical analyses were performed using the R software (cran.r-project.org). Log-shape ratios (Mosimann and James, 1979) were calculated on the $\log_{10}$-transformed measurements. These manipulations allow for the separation of the shape and size components of the variables. Principal component analysis (PCA) was then performed on these log-shape ratios to explore the data. Linear regressions between each axis of the PCA and overall size (the mean of all measurements after $\log_{10}$ transformation for each individual) were performed to check the presence of an allometric component in the data. Finally, we performed linear discriminant analyses (LDA) on the PCA axes and constructed Mahalanobis distance trees to observe the morphological distance between the investigated taxa. Multivariate analyses of variance (MANOVAs) were also carried out to test differences between groups. These analyses were performed using the R libraries MASS (Ripley et al., 2016) and Ape (Paradis et al., 2015). All P values were considered significant if <0.01.

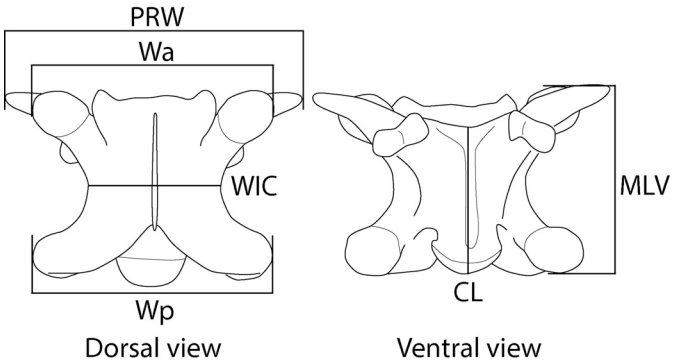

FIGURE 2. Measurements taken on snake vertebrae. **Abbreviations**: **CL**, (greatest) centrum length; **MLV**, maximum length of vertebra; **PRW**, prezygapophyseal width; **Wa**, (greatest) width of the anterior part of the neural arch; **WIC**, width of interzygapophyseal constriction (= 'NAW' sensu Szyndlar, 1984); **Wp**, (greatest) width of the posterior part of the neural arch (= 'PO-PO' sensu Szyndlar, 1984).

The comparative sample used in the morphometric analysis includes three specimens of *Boa nebulosa* (MNHN-ZA-AC 2016.1, MNHN-ZA-AC 2016.2, and MEC-Boa 3) and four specimens of *Boa constrictor* (MCZ 172037, MNHN-ZA-AC 1876-250, MNHN-ZA-AC 1876-618, and MNHN-UMR7209-672). Considering that centrum length and overall morphology of the trunk vertebrae are variable along the column, we measured 15 distinct trunk vertebrae, representing the full morphological variability of the post-'cervical' trunk vertebrae of each specimen.

Estimation of the Length of Fossil Snakes

The length of the fossil snakes was estimated using an equation produced by the results of a linear regression between the natural logarithm of the centrum length (CL) of post-'cervical' trunk vertebrae and the natural logarithm of the total length of comparative *Boa* snakes of known size. This method was previously applied to estimate the size of fossil Lesser Antillean lizards (Bochaton, 2016; Bochaton and Kemp, 2017). The comparative specimens used to build the equation are two of *B. constrictor* (MNHN-ZA-AC 1876-250 and MNHN-UMR7209-672), with respective total lengths of 230 and 74 cm, and three of *B. nebulosa* (MNHN-ZA-AC 2016.1, MNHN-ZA-AC 2016.2, and MEC-Boa 3), with respective total lengths of 64, 114, and 93 cm. Measured vertebrae were the same as those used in the morphometric analysis. The correlation between centrum length and specimen length was strong and significant ($R^2 = 0.94$, $P < 0.01$). The obtained size estimation equation was the following:

$$\text{Total length in cm} = \text{Exponential [ln}$$

$$\text{(centrum length in mm)} \times 0.8749 + 3.42\text{]}$$

However, variability of the size of trunk vertebrae affects the accuracy of snout-to-vent length (SVL) estimations, which present a mean error of 8.5% and a maximum error of 22%.

SYSTEMATIC PALEONTOLOGY

Order SQUAMATA Oppel, 1811
Suborder SERPENTES Linnaeus, 1758
Infraorder ALETHINOPHIDIA Nopcsa, 1923
Family BOIDAE Gray, 1825
BOA BLANCHARDENSIS, sp. nov.

Holotype—A parabasisphenoid bone (Fig. 3A, B): MEC-A-18.1.1.1 from 'layer 10' of Blanchard Cave (Pleistocene; see Bailon et al., 2015).

Referred Material—One maxilla, one prefrontal, one ectopterygoid, three pterygoids, two palatine bones, one quadrate, two supratemporals, one exoccipital, three dentaries, and one compound bone collected in the Pleistocene layers of Blanchard Cave, and 159 trunk vertebrae, 10 'cervical' vertebrae, 29 caudal vertebrae (cloacal vertebrae are absent), and 63 ribs collected in the Pleistocene layers of Blanchard Cave, Cadet 2 cave, and Cadet 3 rock shelter (Figs. 3–6). These remains represent a least four individuals.

Geological Age—Late Pleistocene; 34,000–15,000 BP.

Diagnosis—The following characters were encountered only in *Boa blanchardensis*, sp. nov.: parabasisphenoid with weakly individualized and developed basipterygoid processes (Fig. 3A, B; Fig. S1); weakly medially extended triangular

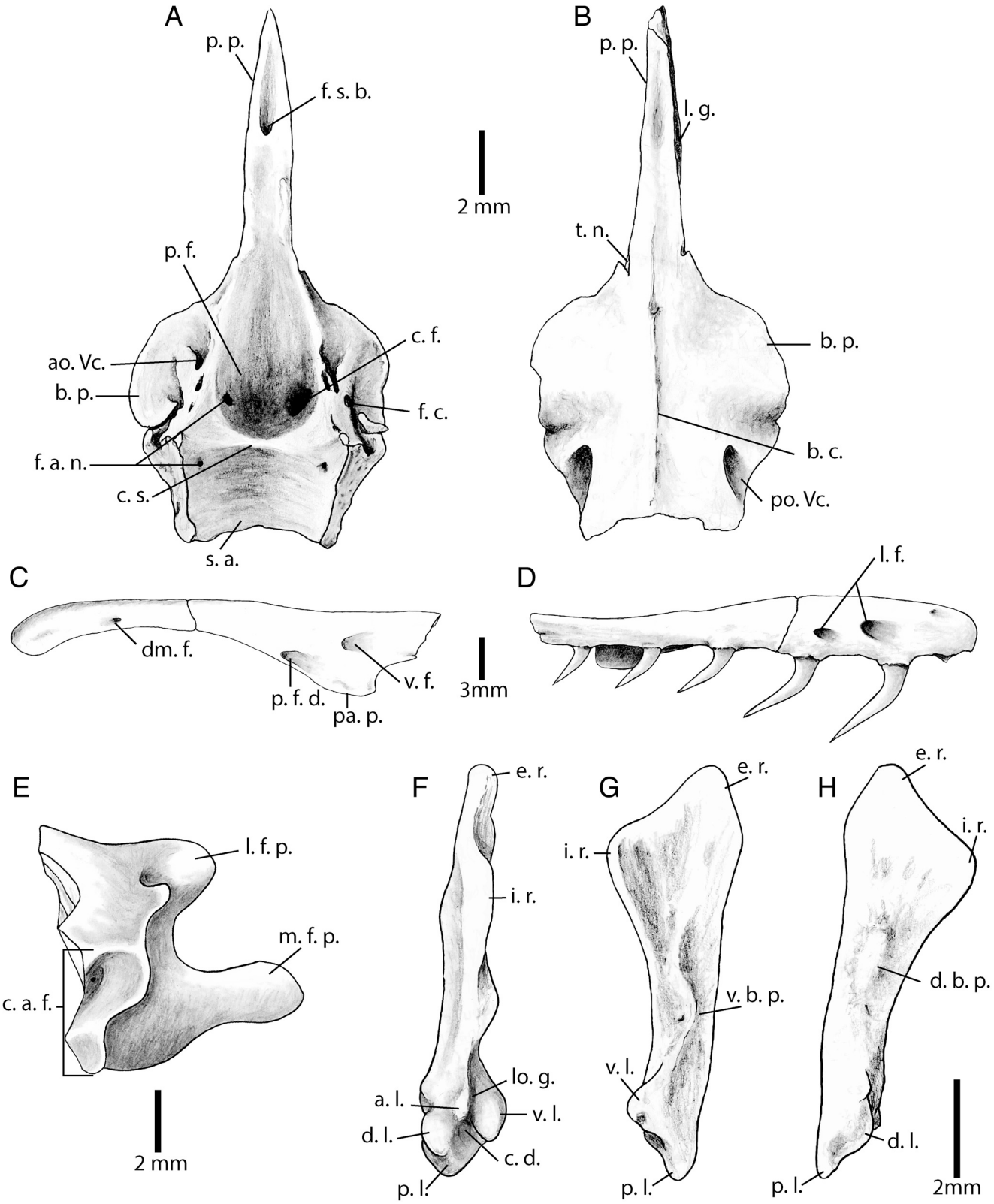

FIGURE 3. *Boa blanchardensis*, sp. nov., cranial elements. **A**–**B**, MEC-A-18.1.1.1, holotype, parabasisphenoid in **A**, dorsal and **B**, ventral views. **C**–**D**, MEC-A-18.1.1.2, right maxilla in **C**, dorsal and **D**, lateral views. **E**, MEC-A-18.1.1.4, right prefrontal in dorsal view. **F**–**H**, MEC-A-18.1.1.5, left ectopterygoid in **F**, medial, **G**, ventral, and **H**, dorsal views. Drawings by S. Bailon. **Abbreviations**: **a. l.**, anterior lobe; **ao. Vc.**, anterior opening of the Vidian canal; **b. c.**, basisphenoid crest; **b. p.**, basipterygoid process; **c. a. f.**, contact area with the frontal bone; **c. d.**, central depression; **c. f.**, carotid foramen; **c. s.**, crista sellaris; **d. b. p.**, dorsal bony protuberance; **d. l.**, dorsal lobe; **dm. f.**, dorsomedial foramen; **e. r.**, external ramus; **f. a. n.**, foramen of the abducens nerve; **f. c.**, foramen for the cid-nerve; **f. s. b.**, foramen of the supratrabecular blade; **i. r.**, internal ramus; **l. f.**, lateral foramina; **l. f. p.**, lateral foot process; **l. g.**, lateral groove; **lo. g.**, longitudinal groove; **m. f. p.**, medial foot process; **p. f.**, pituitary fossa; **p. f. d.**, posterior foramen of the superior dental canal; **p. l.**, posterior lobe; **p. p.**, parasphenoid process; **pa. p.**, palatine process; **po. Vc.**, posterior opening of the Vidian canal; **s. a.**, sphenoid area; **t. n.**, trabecular notch; **v. b. p.**, ventral bony protuberance; **v. f.**, vascular foramen; **v. l.**, ventral lobe.

palatine process of the maxilla (Fig. 3A, B; Fig. S2) and posterior foramen of the superior dental canal well opened in lateral direction in dorsal view; ectopterygoid with a dorsal bony protuberance corresponding to the impression of the postorbital (Fig. 3F–H; Fig. S1); contact area of the ectopterygoid with the pterygoid constituted by a central depression surrounded by four well-developed lobes, and posterior area of this bone weakly incurved (Fig. 3F–H; Fig. S1); pterygoid with two anterior foramina (Fig. 4D, E); posteromedial process of the palatine distally well enlarged, individualized, and extended in lateral direction (Fig. 4F, G; Fig. S1); nearly symmetrical supratemporal (Fig. 5C; Fig. S1); exoccipital with high and posteriorly incurved occipital crest (Fig. 5D); short retroarticular process of the compound bone (Fig. 5G, H; Fig. 2S); and trunk vertebrae with moderately low neural spine.

In addition to these apomorphic characters, differences and similarities to *B. constrictor* and/or *B. nebulosa* were recorded and are discussed in the Comments section, following the description of the material. The characteristics of modern *B. constrictor* and *B. nebulosa* are presented in Figures S1 and S2 in Supplemental Data.

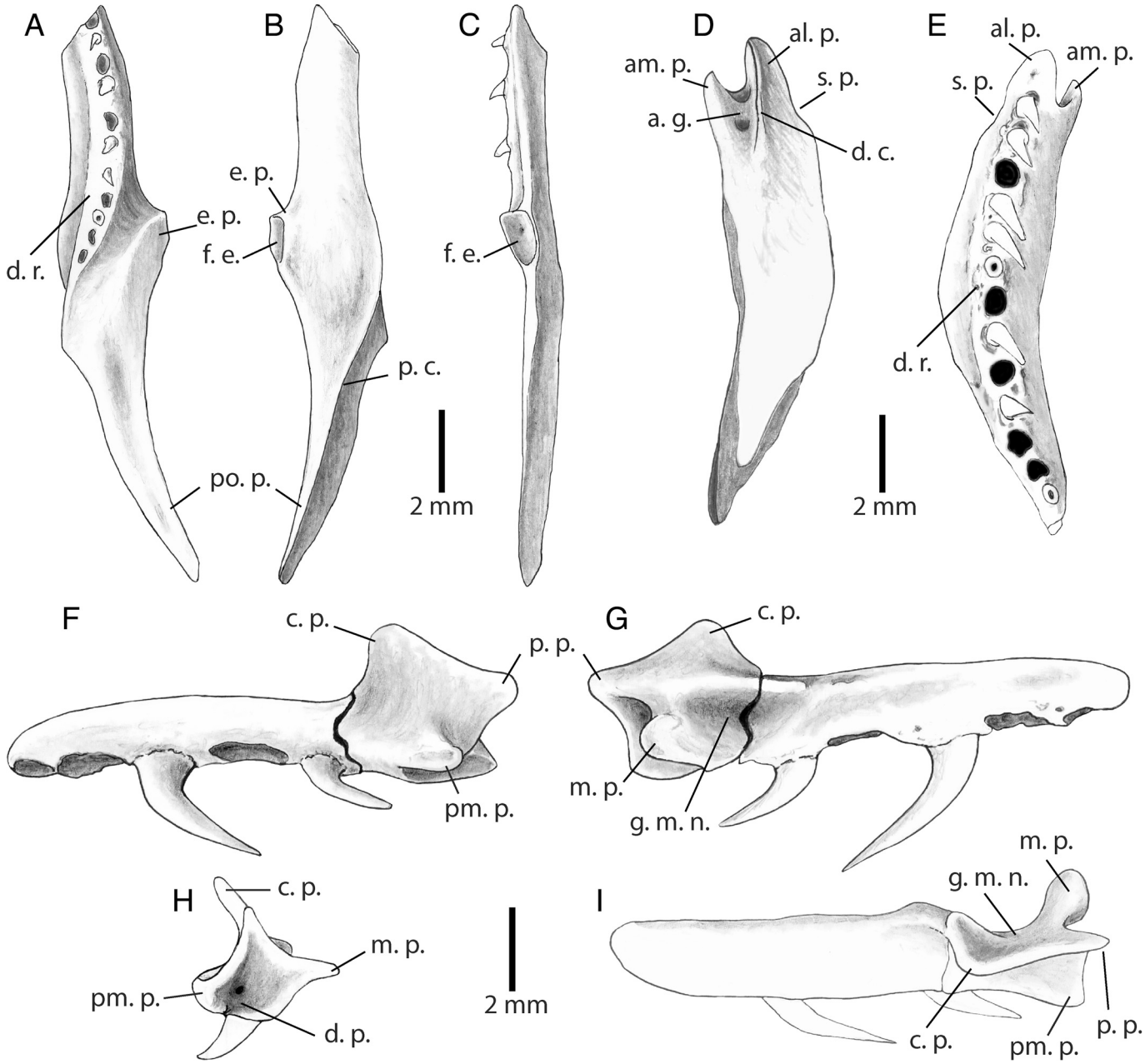

FIGURE 4. *Boa blanchardensis*, sp. nov., cranial elements, from Blanchard Cave. **A**–**C**, MEC-A-18.1.1.6, left pterygoid in **A**, ventral, **B**, dorsal, and **C**, medial views. MEC-A-18.1.1.7, right pterygoid in **D**, dorsal and **E**, ventral views. **F**–**I**, MEC-A-18.1.1.9, right palatine in **F**, medial, **G**, lateral, **H**, posterior, and **I**, dorsal views. Drawings by S. Bailon. **Abbreviations**: **a. g.**, anterior groove for the insertion of the palatal; **al. p.**, anterolateral process; **am. p.**, anteromedial process; **c. p.**, choanal process; **d. c.**, dorsal crest; **d. p.**, depression for the insertion of the anterolateral process of the pterygoid; **d. r.**, dental row; **e. p.**, ectopterygoid process; **f. e.**, facet for the attachment of the ectopterygoid; **g. m. n.**, groove for the passage of the maxillary nerve; **m. p.**, maxillary process; **p. c.**, pterygoid crest; **p. p.**, posterior process; **pm. p.**, posteromedial process; **po. p.**, posterior process; **s. p.**, nick for the insertion of the palatal process of the maxilla.

Etymology—The species epithet '*blanchardensis*' refers to Blanchard Cave, the site from which the holotype material was discovered, and is applied here as a noun in apposition. We propose the English name 'Marie-Galante Boa' and the French name 'Boa de Marie-Galante.'

DESCRIPTION

Parabasisphenoid—The holotype, a complete parabasisphenoid, measures 16.8 mm in length (Fig. 3A, B). The parasphenoid process is long (approximately half of the total length of the bone), thin, and lanceolate. In ventral view, two trabecular notches indicating the position of the trabecular processes (processus trabeculae sensu Hoffstetter, 1939) are present at the base of the parasphenoid process. This latter process is laterally excavated by two lateral grooves ('sulci trabeculae' sensu Hoffstetter, 1939), which give a horizontal 'H' shape to the cross-section of the parasphenoid process. The dorsal (supratrabecular blade) and ventral (infratrabecular blade) margins of the parasphenoid process are slightly concave and of similar widths. A foramen anteriorly prolonged by a furrow occurs on the anterior half of the supratrabecular blade. Also in ventral view, the basisphenoid part of the bone is subpentagonal. The basipterygoid process area is weakly developed and individualized. The basisphenoid crest is long and thin and runs from the posterior margin of the bone to the posterior limit of the parasphenoid process. The posterior openings of the Vidian canal are wide, and the right one is wider than the left one. Each of these openings is posterolaterally extended by a furrow reaching the posterior margin of the bone. The posterior margin of the bone is concave and does not seem to bear any posterior process. In dorsal view, the pituitary fossa (sensu Szyndlar, 1984) is deep and twice as long as wide. The two carotid foramina ('carotis cerebralis' sensu Rieppel, 1979) are clearly visible at the bottom of the pituitary fossa, and the right foramen is wider than the left one. The sphenoid area is reduced, very transversally concave, and forms little of the braincase. It is separated from the pituitary fossa by a crista sellaris. On each lateral side of the crista sellaris, a contact area occurs between the parietal (anterior) and prootic (posterior) bones. The right and left canals of the abducens nerves (VI) (sensu Rieppel, 1979) are opened by two foramina situated posteriorly and anteriorly to the crista sellaris. The anterior openings of the Vidian canal are out of the pituitary fossa and situated at the bases of each basipterygoid process. Posteriorly to these cavities, foramina occur for the cid-nerves (sensu Rieppel, 1979). These latter foramina are posteriorly prolonged by a canal that is open on the right side of the bone and partially closed on the left side. In ventral view, the posterior openings of the Vidian canal are visible in the posterolateral areas of the bone near the joint with the prootic bone.

Maxilla—The only fragment of maxilla, MEC-A-18.1.1.2, corresponds to the anterior half of a right bone (Fig. 3C, D). The maximal length of this bone is 21.1 mm. It is elongated and slightly anteromedially curved in dorsal view. In lateral view, the bone is low and presents a poorly defined suborbital margin, and two wide lateral foramina occur on the anterior half of its lateral margin. The most anterior of these foramina is situated between the fourth and fifth teeth, and the most posterior above the sixth tooth. A dorsomedial foramen occurs at the level of the anterior lateral foramen. In ventral view, the bone bears 11 dental positions occupied by ankylosed-subthecodont teeth occupying the lateral edge of the bone. In lateral view, these teeth present a curved shape. The anterior teeth are the longest, and their size decreases posteriorly. A moderately developed palatine process of subtriangular shape in dorsal view occurs in the posterior part of the fragment. This process presents a long anterior margin and a rounded medial margin and is medioventrally incurved. In dorsal view, two maxillary foramina occur on the dorsal margin of the palatine process: a posterior foramen of the superior dental canal (sensu Anthony and Serra, 1950) in an anteromedial position and a vascular foramen (sensu Anthony and Serra, 1950) in a central position. These two foramina converge in the same internal alveolar canal in which the two lateral foramina also open. The occurrence of an ectopterygoid process cannot be assessed.

Prefrontal—The only prefrontal fragment, MEC-A-18.1.1.4, corresponds to the posterior part of a right bone (Fig. 3E). In dorsal view, the bone presents a well-developed and individualized spoon-shaped medial foot process and a well-developed and individualized lateral foot process, slightly shorter than the medial foot process and presenting a rounded apex. Also in dorsal view, a slight contact area with the frontal bone is visible. The prefrontal lacrimal duct roof is absent. In ventral view, a small foramen occurs at the base of the lateral foot process.

Ectopterygoid—The only recovered ectopterygoid, MEC-A-18.1.1.5, is a complete left bone with a maximal length of 8.3 mm (Fig. 3F–H). This bone is elongated and robust. In dorsal view, the anterior extremity is asymmetric, with a subtriangular external ramus that is more developed than the internal ramus. The bony blade linking these two processes is very slightly concave. Two bony protuberances occur on the dorsal and ventral surfaces of the bone: they correspond to the imprints of, respectively, the postorbital and the ligaments of the distal extremity of the maxilla. The posterior extremity of the bone is well ossified. In medial view, the contact area with the pituitary fossa of the pterygoid bears four lobes (anterior, posterior, dorsal, and ventral), surrounding a central depression. The ventral and anterior lobes are separated by a longitudinal groove prolonged anteriorly to the base of the ventral bony protuberance.

Pterygoid—The three fragments of pterygoid recovered (one left and two right bones) correspond to the anterior (MEC-A-18.1.1.7), median (MEC-A-18.1.1.8), and posterior/median (MEC-A-18.1.1.6) parts of the bone and record the whole morphology of the bone (Fig. 4A–E). The anterior margin of the bone is divided into two processes. The first process is a short anteromedial process of suboval shape in medial view, slightly anteroventrally incurved in lateral view, and lateromedially flattened in dorsal view. The second process is an anterolateral process that is twice as long as the anteromedial process and with a prominent dorsal crest. These two processes are separated by a deep anterior groove corresponding to the insertion of the palatine. Two anterior foramina are visible at the bottom of the anterior groove. Also in ventral view, the anterolateral margin of the bone presents a small nick for the insertion of the palatal process of the maxilla. In dorsal view, the bone presents a high and sigmoid pterygoid crest (sensu Szyndlar, 1984) diagonally crossing the posterior half of the bone. This crest extends anteriorly beyond the level of the ectopterygoid process on the medial edge of the bone. In ventral view, the bone bears a short ectopterygoid process, presenting a lateral facet for the attachment of the ectopterygoid visible only in lateral view. This facet is concave, subtriangular, and with a closed boundary in lateral view. A slightly over-elevated arched dental row, bearing 13 tooth positions in the most complete fragment, is also visible in ventral view on the anterior half of the bone. The lateral side of the dental row is pierced by at least two foramina. The posterior part of the bone lacks teeth and is prolonged by a long and slender posterior process with a pointed posterior tip. At the base of this process lies an ovoid groove of moderate depth.

Palatine—The most complete palatine, MEC-A-18.1.1.9, is a right bone with a maximal length of 13.5 mm (Fig. 4F–I). The bone is elongated and bears five tooth positions. The anterior teeth are longer than the posterior ones. In dorsal view, the maxillary process is well individualized, short, oriented in a lateral direction, and in a posterolateral position near the posterior extremity of the bone and the junction with the pterygoid. Also

in dorsal view, the extremity of this process is enlarged and circular. The choanal process is moderately developed and occupies the posterior third of the total length of the bone. This process is triangular and inclined in medial direction at an angle of around 30°. The choanal process is posteriorly linked to the well-developed posterior process, which is more posteriorly extended than the maxillary process. The posteromedial process is short and poorly individualized. It bears a small posterodorsal notch corresponding to the imprint of the anteromedial process of the pterygoid. The posteromedial process is linked to the posterior process by a slightly concave crest, and the posterior process is linked to the maxillary process by a strongly concave crest. In lateral view, a groove for the passage of the suborbital maxillary nerve occurs anterior to the maxillary process. A foramen is present at the bottom of this groove on MEC-A-18.1.1.10. In posterior view, the bone has an asymmetrical lozenge shape, with a deep depression for the insertion of the anterolateral process of the pterygoid on the living animal. Also in posterior view, the maxillary process is thinner, more elongated, and occupies a more dorsal position than the posteromedial process.

Quadrate—The only recovered element, MEC-A-18.1.1.11, is an almost complete left quadrate bone, with a maximal height of 10.7 mm (Fig. 5A, B). In lateral view, the bone is slightly twisted with a cephalic condyle forming an angle of around 70° in

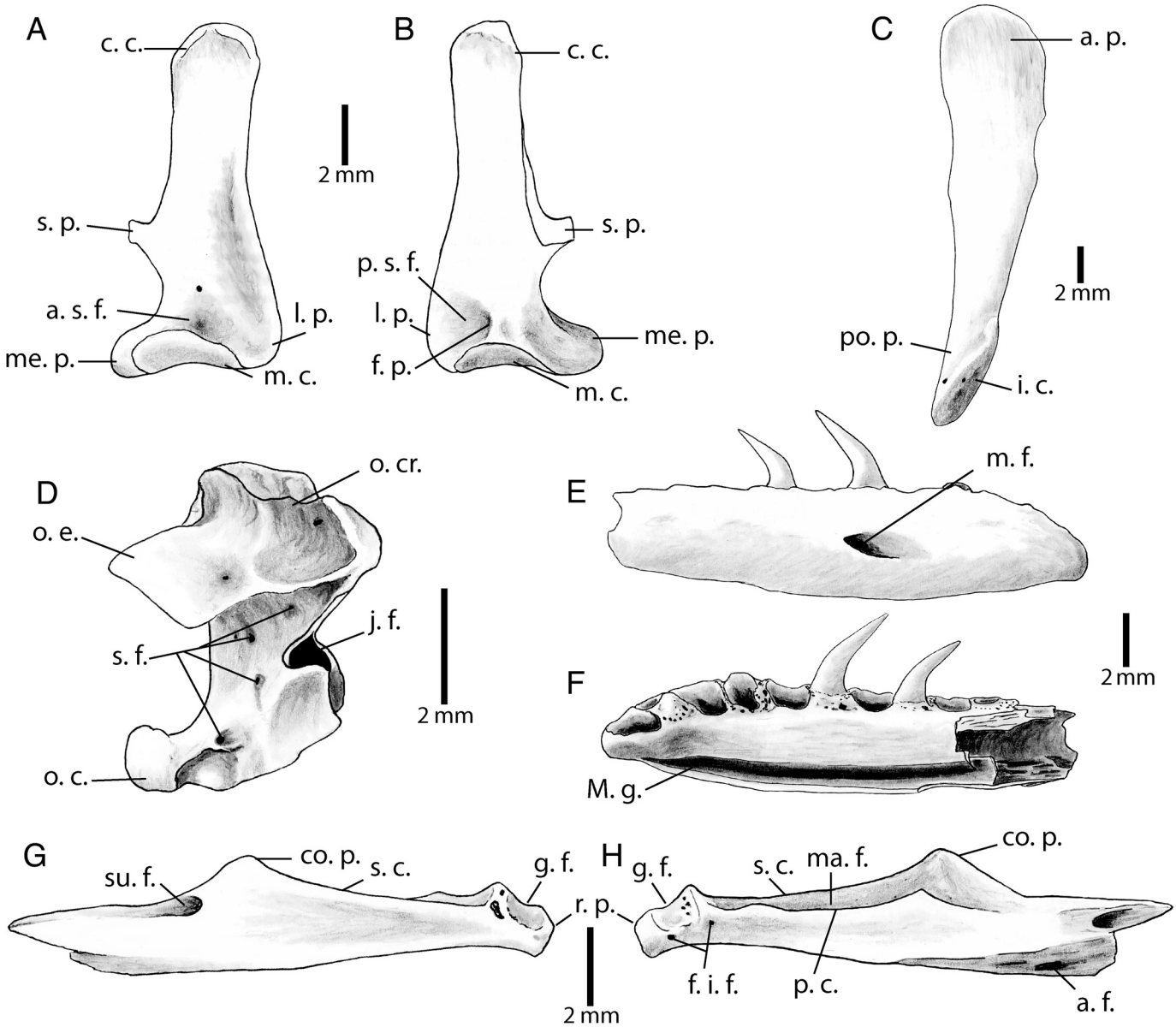

FIGURE 5. *Boa blanchardensis*, sp. nov., cranial and mandibular elements from Blanchard Cave. **A**–**B**, MEC-A-18.1.1.11, left quadrate in **A**, anterior and **B**, posterior views. **C**, MEC-A-18.1.1.16, right supratemporal in dorsal view. **D**, MEC-A-18.1.1.17, right exoccipital in posterolateral view. **E**–**F**, MEC-A-18.1.1.12, right dentary in **E**, lateral and **F**, medial views. **G**–**H**, MEC-A-18.1.1.15, left compound bone in **G**, lateral and **H**, medial views. Drawings by S. Bailon. **Abbreviations**: **a. f.**, anterior foramen; **a. p.**, anterior part; **a. s. f.**, anterior supracondylar fossa; **c. c.**, cephalic condyle; **co. p.**, coronoid process; **f. p.**, foramen of the posterior supracondylar fossa; **f. i. f.**, foramina of the infraglenoid fossa; **g. f.**, glenoid fossa; **i. c.**, imprint of the cephalic condyle; **j. f.**, jugular foramen; **l. p.**, lateral process; **m. c.**, mandibular condyle; **m. f.**, mental foramen; **M. g.**, Meckel's groove; **ma. f.**, mandibular fossa; **me. p.**, medial process; **o. c.**, occipital condyle; **o. cr.**, occipital crest; **o. e.**, opisthotic-exoccipital eave; **p. c.**, prearticular crest; **p. s. f.**, posterior supracondylar fossa; **po. p.**, posterior part; **r. p.**, retroarticular process; **s. c.**, surangular crest; **s. f.**, small foramen; **s. p.**, stapedial process; **su. f.**, surangular foramina.

relation to the mandibular condyle. The cephalic condyle is weakly enlarged. In dorsal view, the cephalic condyle is suboval, with a weak central constriction and a wider anterolateral extremity. In ventral view, the mandibular condyle is shaped like a transversally elongated saddle. This condyle is bordered laterally by a short, rounded lateral process and medially by a rounded but longer medial process that is more individualized than the lateral process. In anterior view, a shallow subtriangular anterior supracondylar fossa occurs. In posterior view, the posterior supracondylar fossa is deep, of subcircular shape, and slightly off-center on the lateral side of the bone. The imprint of the posterior process of the pterygoid occupies the entire posterior surface of the medial process. On the ventral third of its medial edge, the bone bears a well-developed and individualized stapedial process partially preserved on the fossil. The medial border of the bone between the stapedial process and the cephalic condyle is also broken. Two foramina occur on the bone: a first at the bottom of the posterior supracondylar fossa and a second on the apex of the anterior supracondylar fossa.

Supratemporal—MEC-A-18.1.1.16 is spatula-shaped (Fig. 5C). It is elongated, with a flat and rounded, but slightly asymmetrical anterior part. Its posterior part is narrower but thicker and bears an oval imprint of the cephalic condyle of the quadrate on its lateral side.

Exoccipital—The only recovered exoccipital, MEC-A-18.1.1.17, is a mostly complete bone with a partly broken anterior part (Fig. 5D). The bone exhibits a well-developed dorsolateral occipital crest, with a posterior curve marking the contact area with the prootic bone. The anterolateral margin of the bone corresponds to the opening of the jugular foramen (sensu Rieppel and Zaher, 2001). Posterior to that opening, several smaller foramina, possibly corresponding to the roots of the hypoglossal nerve, are visible on the lateral surface of the bone. The opisthotic-exoccipital eave (sensu McDowell, 2008) is well developed but does not extend posteriorly beyond the level of the occipital condyle.

Dentary—Specimens MEC-A-18.1.1.12, MEC-A-18.1.1.13, and MEC-A-18.1.1.14 represent three anterior and posterior fragments (two right fragments and one left). The largest fragment, MEC-A-18.1.1.12, represents the anterior half of the bone and bears 11 tooth positions, but the number of dental positions of the whole bone cannot be assessed clearly (Fig. 5E, F). In medial view, this bone is robust and presents a narrow Meckel's groove that does not reach the anterior extremity of the dentary. The morphology of the teeth is similar to that of the maxilla, and their size also seems to be progressively decreasing, at least in the posterior part of the dentary. In lateral view, the bone bears a large mental foramen in its anterior part.

Compound Bone—The only compound bone recovered is MEC-A-18.1.1.15, a nearly complete left bone with a maximum length of 14.2 mm (Fig. 5G, H). The bone is elongated and presents a blunt, very short retroarticular process, slightly oriented in ventromedial direction. In lateral view, the bone presents a low surangular crest in the posterior part and is anteriorly prolonged by a high, triangular, and pointed coronoid process. This last process presents a slight anteromedial impression of the coronoid bone. A large surangular foramen occurs below the anterior extremity of the surangular crest, and an impression of the posteroventral process of the dentary occurs in the anteroventral area of the bone. In medial view, the prearticular crest is broken on the sole available specimen but was at least as high as, and probably higher than, the posterior part of the surangular crest. Two foramina occur below the glenoid fossa. A deep impression of the angular pierced by an anterior foramen occurs in the anteroventral area of the bone. In dorsal view, the mandibular fossa is long and moderately wide; its anterior part is occupied by a very large foramen extending in an anterior direction.

Trunk Vertebrae—Of the 159 elements, two (MEC-A-18.1.1.19 and MEC-A-18.1.1.20) are illustrated here (Fig. 6). They are strongly built, with a centrum length varying between 2.7 and 5.7 mm. In dorsal view, these vertebrae are wider than long (ratio CL/WIC = 0.69–0.89). In dorsal view, the zygosphene presents a moderately to very concave anterior margin, the neural arch is short, and the condyle is visible. Prezygapophyseal processes are, in most cases, extremely short and hidden below the prezygapophysis in dorsal view (Fig. 6F) but are, in small specimens, weakly developed and visible in dorsal view (Fig. 6A). Prezygapophyseal facet shape ranges from ovoid on small vertebrae (Fig. 6A) to a rectangular on larger specimens (Fig. 6F); they are also shorter and more anterolaterally oriented than in large vertebrae, on which prezygapophyseal facets are extended in a lateral direction. The posterolateral margins of the neural arch are straight. The posterior notch of the neural arch is anteroposteriorly flared and forms an angle of around 90°. In lateral view, the morphology of the neural spine varies from nearly as high as long to clearly higher than long; its posterior margin is posteriorly inclined. Also in lateral view, the neural arch is high and narrow and a lateral foramen housed in a shallow depression

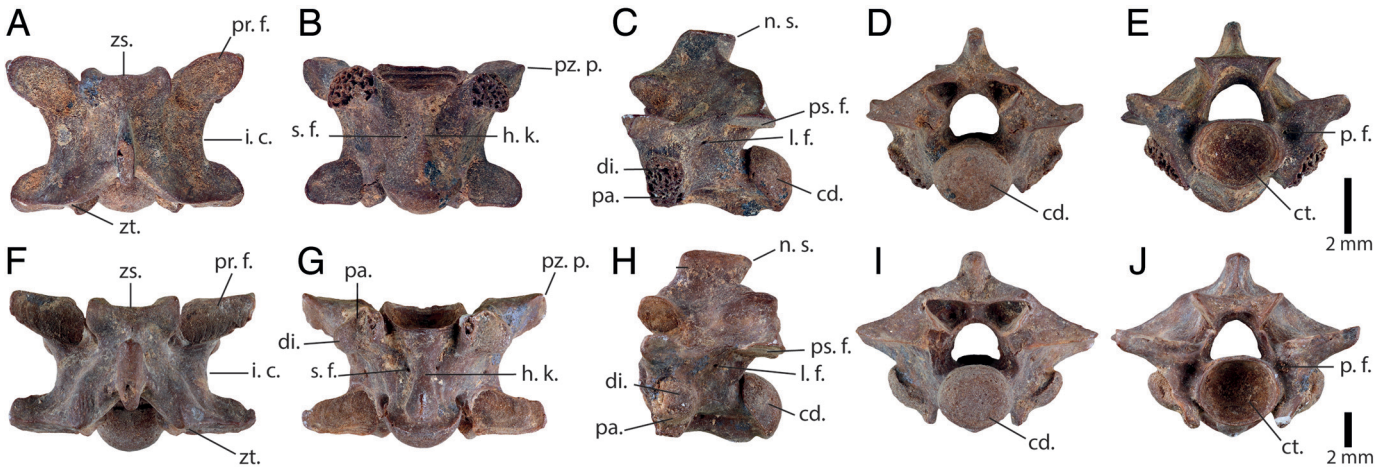

FIGURE 6. *Boa blanchardensis*, sp. nov., trunk vertebrae from Blanchard Cave. **A**–**E**, MEC-A-18.1.1.19, small vertebra in **A**, dorsal, **B**, ventral, **C**, lateral, **D**, posterior, and **E**, anterior views. **F**–**J**, MEC-A-18.1.1.20, large vertebra in **F**, dorsal, **G**, ventral, **H**, lateral, **I**, posterior, and **J**, anterior views. **Abbreviations**: **ct.**, cotyle; **cd.**, condyle; **di.**, diapophysis; **h. k.**, hemal keel; **i. c.**, interzygapophyseal constriction; **l. f.**, lateral foramen; **n. s.**, neural spine; **pa.**, parapophysis; **p. f.**, paracotylar foramen; **pr. f.**, prezygapophyseal facet; **ps. f.**, postzygapophyseal facet; **pz. p.**, prezygapophyseal process; **s. f.**, subcentral foramen; **zs.**, zygosphene; **zt.**, zygantrum.

is present. In ventral view, the condyle presents a well-marked precondylar constriction. Subcentral foramina occur on both sides of the hemal keel. The centrum is triangular, with a thin to wide hemal keel showing a blunted ventral edge. The variability of the morphology of the hemal keel from wide with weakly delimited concave margins to thin with straight, well-delimited margins could be related to the position of the vertebra in the column, from median to posterior precloacal positions, as observed in modern *Boa* specimens. The paradiapophysis presents a diapophysis that is weakly individualized from the parapophysis. Postzygapophyseal facets are of ovoid to rectangular shape. In anterior view, the zygosphene is thick and as wide as, to clearly wider than, the cotyle. The cotyle is large, oval, and slightly wider than high. The prezygapophysis is slightly inclined in a medial direction. Paracotylar depressions occur on each side of the cotyle, and a paracotylar foramen occurs in each of them. In posterior view, the condyle is oval and slightly wider than high. The neural canal is subtriangular and nearly two times wider than high. The neural arch is thick and strongly built.

'Cervical' and Caudal Vertebrae—A total of 39 elements are known. These vertebrae are similar to those previously described, but the 'cervical' vertebrae exhibit long and thin hypapophyses extending in a posteroventral direction, or a posterior projection of the hemal keel in the most posterior 'cervical' vertebrae. The caudal vertebrae are longer and present hemapophyses, pleurapophyses, or lymphapophyses. These vertebrae present significant morphological variability, and their detailed morphology is thus not taken into account for the identification of the fossil.

Ribs—Sixty-three rib elements were associated with this taxon on the basis of their size and on account of the fact that their capitular (dorsal) and tubercular (ventral) articular facets are less individualized than in the Colubroidea. They also lack tuberculiform processes.

Comments

These remains present several characteristics of boine snakes: the occurrence of a short maxillary process of the palatine near the posterior extremity of the bone and the presence of a groove for the passage of the suborbital maxillary nerve (Cundall and Irish, 2008); a pterygoid exhibiting a lateral impression of the ectopterygoid (Kluge, 1991); a parabasisphenoid presenting a Vidian canal separated from the cranial cavity (Rieppel, 1979), and a right opening of the Vidian canal larger than the left one (Underwood, 1976); and the occurrence of a prearticular crest at least as high as, but probably higher than, the surangular crest on the compound bone (Cundall and Irish, 2008). In addition, the vertebrae preserve a combination of morphological characteristics occurring in boines: they are strongly built, high, short, and wide, with an undepressed neural arch that has a strongly notched posterior margin, a thick zygosphene, low inclination of the articular facet of the prezygapophyses, short prezygapophysial process, a vertebral centrum shorter than neural arch width, well-defined precondylar constriction, paradiapophyses weakly subdivided, and hemal keel in all post-'cervical' trunk vertebrae (Rage, 2001; Szyndlar and Rage, 2003; Hsiou and Albino, 2009; Albino, 2011). These vertebrae also all bear small paracotylar foramina, a concave anterior edge of the zygosphene in dorsal view, and a zygosphene wider than the cotyle, which are characters occurring in *Boa* (Albino, 2011, 2012).

Differences between *B. constrictor* and *B. nebulosa/B. blanchardensis,* sp. nov—*Boa blanchardensis*, sp. nov., shares several characteristics with *B. nebulosa* that differentiate them from the continental *B. constrictor*. The cross-section of the parasphenoid process of the parabasisphenoid of *B. constrictor* is 'I'-beam-shaped, whereas it is horizontal and 'H'-shaped in both *B. blanchardensis*, sp. nov., and *B. nebulosa*. On the same bone, the ventral margin of the parasphenoid process (infratrabecular blade) on some *B. constrictor* specimens can be reduced to a vertical ventral crest posteriorly prolonged by the basisphenoid crest, whereas this condition does not occur in other investigated taxa. The external ramus of the anterior extremity of the ectopterygoid is more developed than the internal ramus in *B. blanchardensis*, sp. nov., and modern *B. nebulosa*, whereas these two rami are of comparable development in *B. constrictor* (Fig. 3F–H; Fig. 1S). The pterygoid of *B. constrictor* presents an anteriorly open articular facet with the ectopterygoid in lateral view, whereas the boundary of this facet is closed in *B. blanchardensis*, sp. nov., and *B. nebulosa* (Fig. 2S). The *B. constrictor* quadrate bears a truncated lateral process and a shorter medial process than in other observed *Boa* (Fig. 2S). On the same bone, the anterior supracondylar fossa is very shallow or nearly absent in *B. constrictor* but well marked in *B. blanchardensis*, sp. nov., and *B. nebulosa* (Fig. 2S). Concerning the trunk vertebrae, in most vertebrae of *B. blanchardensis*, sp. nov., and *B. nebulosa*, the neural spine is also clearly lower than in continental specimens.

Differences between *B. nebulosa* and *B. blanchardensis*, sp. nov—*Boa blanchardensis*, sp. nov., differs from *B. nebulosa* in the following aspects: the pterygoid of the fossil presents an ectopterygoid facet of subtriangular shape, whereas it is kidney-shaped in *B. nebulosa* (Fig. 2S). On the same bone, the lateral margin of the posterior process is more concave in *B. nebulosa* than in *B. blanchardensis*, sp. nov. (Fig. 2S). The prefrontal of *B. blanchardensis*, sp. nov., presents a slightly longer spoon-shaped medial foot process than the lateral foot process, whereas in *B. nebulosa* the medial foot process is slender and pointed and twice as long as the lateral foot process (Fig. 2S). The palatine of the fossil presents a longer and more individualized posterior projection than in *B. nebulosa* (Fig. 2S). The compound bone of *B. blanchardensis*, sp. nov., lacks the long foramen of the prearticular crest occurring on the medial side of the bone on all our *B. nebulosa* and some of our *B. constrictor* specimens (Fig. 2S). The vertebrae of *B. blanchardensis*, sp. nov., also present a strongly concave anterior margin of the zygosphene in dorsal view, whereas this is straight in *B. nebulosa*. This character, absent in our comparative material of *B. constrictor*, was reported to also occur in continental *Boa* (Albino and Carlini, 2008; Albino, 2011; Onary-Alves et al., 2016), showing that both character states occur in *Boa constrictor*.

Characters Exclusive to *B. blanchardensis*, sp. nov—The fossil also presents several characters that we did not record in any other *Boa* specimens. These characters are listed above in the Diagnosis section.

Ontogenetic and Size Characteristics of *B. blanchardensis*, sp. nov—Observations of the largest mid-trunk vertebrae of comparative specimens allowed us to define vertebral characters subject to ontogenetic variability in *B. nebulosa*. Indeed, the mid-trunk vertebrae of smaller specimens present the following differences from those of the larger specimens: a very short centrum (below 4 mm of length), weak interzygapophyseal constriction related to a more anterior orientation of the prezygapophyses and to a more posterior orientation of the postzygapophyses than in larger specimens, shorter neural spine, a cotyle and a condyle clearly wider than high, and longer and thinner prezygapophyseal processes. In addition, the shapes of the prezygapophyseal and postzygapophyseal facets appear to vary from ovoid in smaller specimens to rectangular in larger specimens (previously observed by Auffenberg, 1963). With regard to these characters, most of our fossil vertebrae seem to present adult morphologies. Some of the characters we considered as 'juvenile characters' also occur on smaller posterior trunk vertebrae of adult *B. constrictor* (Albino, 2011). As a consequence, we are not able to confirm the occurrence of juvenile specimens in the fossil material. These observations are interesting when compared with the indications provided by the centrum length measurements of the fossil vertebrae and the size estimation equation, indicating that the total

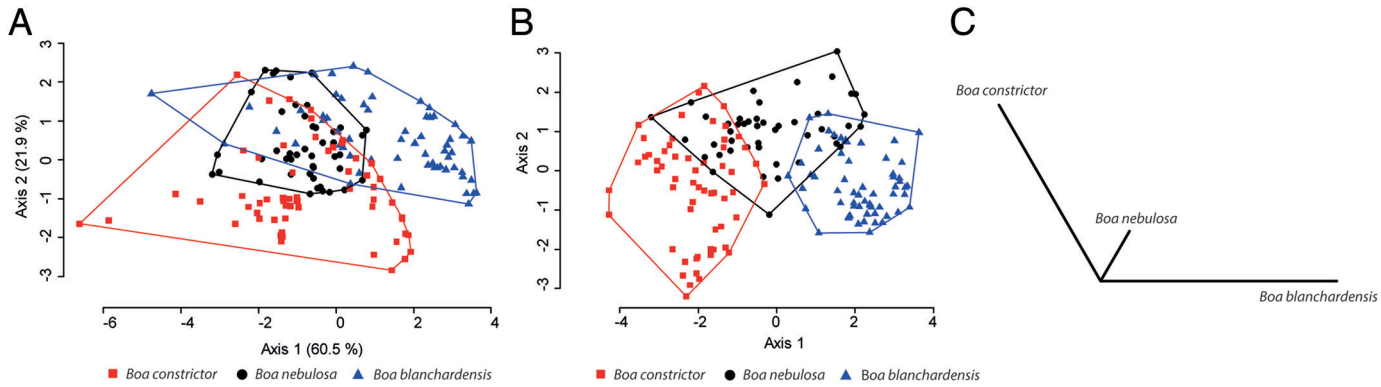

FIGURE 7. **A**, principal component analysis performed on log-shape ratios of the measurements taken on modern and fossil *Boa* trunk vertebrae. **B**, linear discriminant analysis performed on the axis of the PCA. **C**, Mahalanobis distance tree constructed on the results of the PCA.

lengths of *B. blanchardensis*, sp. nov., specimens were between 73 and 139 cm, or between 67 and 151 cm if the average estimation error of the equation is applied to extreme values. This variability could not reflect the variability of the size of trunk vertebrae in a single specimen. Indeed, the largest estimation error recorded for the equation (22%) indicates that there is no overlap between the maximum size estimation variability of the largest (108–170 cm) and smallest (57–89 cm) measured vertebrae.

Morphometric Analysis

The results obtained from the PCA performed on log-shape ratios of modern and fossil *Boa* trunk vertebrae (Fig. 7A) clearly indicate a strong morphological overlap between *B. constrictor*, *B. nebulosa*, and *B. blanchardensis*, sp. nov. However, a MANOVA conducted on the results of this PCA indicates that the three groups are significantly different (MANOVA, $P < 0.01$ and pairwise comparisons all with $P < 0.01$). These differences do not result from allometry effects because linear regressions between axes and overall size indicate a weak allometric component in the PCA axes ($R^2 = 0.29$ and 0.16 for axes 1 and 3 but below 0.04 for all others; $P < 0.01$ for all correlations, except axis 5, which presents a very weak R^2).

Results of the LDA analysis (Fig. 7B) of the PCA and the Mahalanobis distance tree constructed (Fig. 7C) corroborate this finding and show that the fossil is as distant from *B. nebulosa* as from the continental representative of *Boa*. These results complete previous morphological observations and are additional evidence of the morphological differences between *B. blanchardensis*, sp. nov., and its modern relatives.

Skeletochronology

Transverse cross-sections of the three fossil vertebrae prepared for paleohistological observations revealed that they are made of a peripheral layer of parallel-fibered tissue and an internal layer of highly remodeled true lamellar bone with several Howship's lacunae. This observation is valid for the centrum and the neural spine, but the neural arch of the vertebrae appears to be formed of compact parallel-fibered bone. This pattern does not differ from that observed in other squamates (Houssaye et al., 2010, 2013).

The parallel-fibered bone occurring in the neural arch presents putative growth lines marked in polarized light as alternating dark and light lines (Fig. 8). These alternations are frequent in the three sectioned vertebrae (22 or 23 alternations on each vertebra) and could possibly provide information concerning the age of the specimens. However, these marks are not very clear and are difficult to follow around the vertebrae, which implies that some of them could be visual artifacts. In addition, their thickness is very variable and they do not seem to follow a strict cyclicity. The thickness of these marks tends to decrease from a mean of 41.8–71 microns for the five innermost marks to a mean of 21.8–38 microns for the five outermost marks. This could indicate that the growth of the specimens had already started to slow down at the time of death. However, we lack appropriate comparative samples to clearly understand the meaning of our observations in terms of growth dynamics. Thus, although these histological comments allow us to state that our fossils are not juvenile specimens, they are insufficient to demonstrate whether the specimens are young or old adults and whether they were still far from their maximum size or not.

DISCUSSION

Was *B. blanchardensis*, sp. nov., a Dwarf Boid?

Our detailed morphological analysis of *Boa* remains from Marie-Galante, along with morphometric data, indicates that this fossil snake differs in several aspects from the modern *Boa* representative (*B. nebulosa*) on the neighboring island of Dominica and from the mainland *B. constrictor*. These differences allow us to identify this snake as a distinct species: *Boa blanchardensis*, sp. nov. The small size of this snake, highlighted by previous studies (Bailon et al., 2015; Bochaton et al., 2015b), is confirmed by our size estimation equations indicating total lengths between 73 and 139 mm for the fossil specimens. The small size of the specimens was considered in relation to their adult morphology and paleohistological evidence, indicating that growth had already started to slow down despite their small size, which could indicate the proximity of a growth asymptote (Andrews, 1982). However, we lack the appropriate modern comparative sample to interpret the paleohistological results, and although the growth indicated by the fossil was slow, it could still be far from over. This would imply that the largest specimens are absent from our fossil deposits.

The bone deposits in which the *Boa* remains were discovered probably formed as a result of raptors capturing prey and leaving their remains in cave resting sites (Bailon et al., 2015). However, the size of the *Boa* fossil remains is far greater than those of other vertebrates collected in the three investigated deposits (Stouvenot et al., 2014; Bailon et al., 2015; Bochaton et al., 2015b), and the absence of breakage and digestion traces on these remains raises doubts about their prey status (Bailon et al., 2015). Their occurrence in caves most likely reflects predation on bats by *Boa* snakes, which is known to be common in mainland *Boa* (Thomas, 1974) and was also observed in *B. nebulosa* from Dominica (Angin, 2014) and *Boa orophias* from Saint Lucia (Arendt and Anthony, 1986). This hypothesis, provides no obvious explanation for the absence of large specimens in cave deposits because this hunting activity is not restricted to small

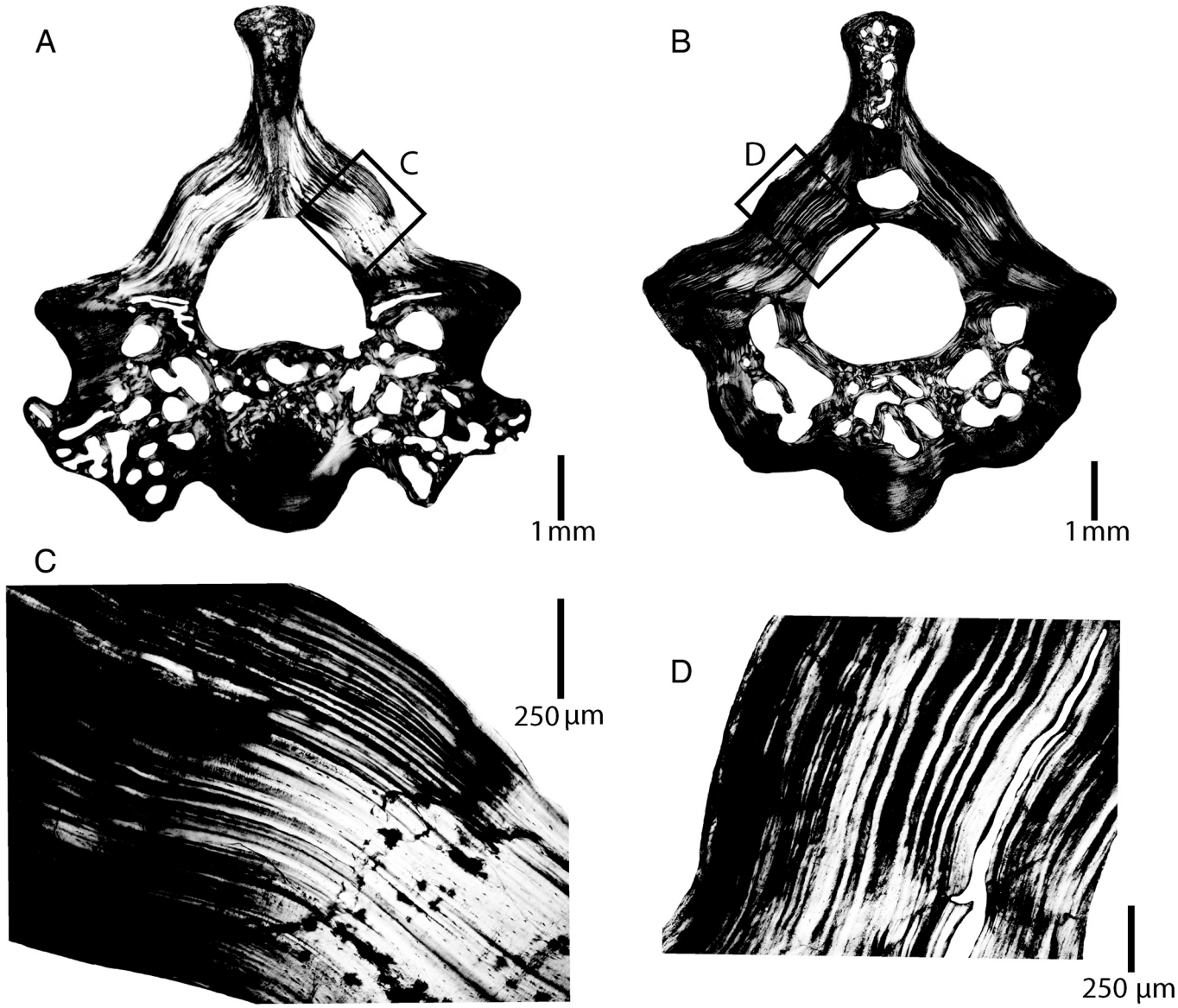

FIGURE 8. **A**, **B**, transverse sections of two fossil *Boa* vertebrae from Pleistocene 'layer 8' of Blanchard Cave (square H32–dec 31). **C**, **D**, details of the parallel-fibered bone layers of the neural arch. Locations of **C** and **D** are indicated on **A** and **B**, respectively, by the open rectangles.

Boa specimens (Angin, 2014). The size of insular snakes is known to be strongly influenced by the size of available prey (Boback, 2003; Boback et al., 2003; Keogh et al., 2005; Tanaka, 2011), and the dwarf status of the Marie-Galante specimens could be easily explained by the lack of large terrestrial prey, as indicated by the Marie-Galante fossil record (Stouvenot et al., 2014; Bailon et al., 2015; Bochaton et al., 2015b; Stoetzel et al., 2016). Consequently, although this could not be unambiguously demonstrated, it is likely that *Boa blanchardensis*, sp. nov., was a dwarf *Boa* species, comparable in size to the dwarf *B. constrictor* of Belize (Boback, 2006). Regardless of whether it was dwarf or not, this snake appears to have been the largest terrestrial vertebrate on Marie-Galante Island during the Pleistocene epoch.

Why Did *B. blanchardensis*, sp. nov., Become Extinct?

Boa blanchardensis, sp. nov., suddenly disappeared from the Holocene age layers of Marie-Galante fossil deposits (Stouvenot et al., 2014; Bailon et al., 2015; Bochaton et al., 2015b) and is also absent from all the archeological deposits of the islands (C. B., pers. observ.). This disappearance is very interesting because no other Marie-Galante squamate taxa appear to have gone extinct at the end of the Pleistocene. The extinction of a colubrid snake on Marie-Galante was mentioned by Bochaton et al. (2015b) and Bailon et al. (2015), but this snake has since been discovered in pre-Columbian Holocene archeological deposits (C.B., pers. observ.). At the end of the Pleistocene, Marie-Galante Island was 71% larger than it is now and supported much drier vegetation (Stoetzel et al., 2016; Royer et al., 2017). The island became smaller and wetter during the Holocene as a consequence of the climatic modifications occurring during this period. This led to a turnover and a depletion of the Marie-Galante bat biodiversity (Stoetzel et al., 2016) but had no apparent effect on terrestrial vertebrates (Bochaton et al., 2015b, 2017b), with the exception of *Boa blanchardensis*, sp. nov. Thus, there is no detectable change in vertebrate prey availability for our *Boa* in the fossil record, and only the size of the island seems to have changed since the Pleistocene. In addition, other snakes

(colubrids) that were similar in size to *B. blanchardensis*, sp. nov., survived throughout the Holocene. However, Boback (2006) stated that dwarf *Boa* adopt a more arboreal way of life, a phenomenon also observed in other dwarf snakes (Luiselli et al., 2015), which feed mainly on birds, and that could result in an important trophic difference compared with fossil colubrid snakes that did not become arboreal. Consequently, the extinction of *Boa blanchardensis*, sp. nov., may be related to a modification in the mostly unknown fossil bird biodiversity of Marie-Galante Island. This hypothesis is even more plausible considering that hurricanes, which are very frequent in the Caribbean (Walker et al., 1991), seem to have a stronger impact on birds (Waide, 1991) than on the other vertebrate taxa occurring on Marie-Galante during the Pleistocene: lizards (Reagan, 1991; Waide, 1991) and bats (Pedersen et al., 1996). However, this hypothesis cannot be tested because bird fossil remains are scarce in fossil deposits and have never been fully investigated (Gala and Lenoble, 2015). Still, a general rarefaction of prey may have had a stronger impact on *B. blanchardensis*, sp. nov., due to its inability to evolve smaller size, considering that it may already have attained the lower size limit for a *Boa* snake. The extinction of *Boa blanchardensis*, sp. nov., remains difficult to explain. However, future, enhanced knowledge of Marie-Galante fossil bird biodiversity and evolution throughout time may contribute to answering this question. Although lacking evidence, there is still a possibility that *Boa* snakes occurred on Marie-Galante Island during the Holocene, but for now this hypothesis is not supported by any physical evidence.

Boa Snakes in Guadeloupe

Apart from *B. blanchardensis*, sp. nov., there is no clear evidence of the past occurrence of a *Boa* snake on the Guadeloupe islands. This possibility is, however, considered to be likely because these snakes are known to occur or to have occurred in the past on several islands south and north of Guadeloupe, which means that this latter archipelago represents a gap in the past distribution of boid snakes across the Lesser Antilles. Still, in contrast to the islands of Martinique (Labat, 1724; Breuil, 2009), Saint Vincent (Moreau de Jonnès, 1816), and Dominica (Anonyme de Carpentras, 1618; Labat, 1724), none of the historical chroniclers describing past Guadeloupe snakes (Du Tertre, 1654; Rochefort, 1658) ever described a *Boa* snake. There is consequently a possibility that *Boa* snakes went extinct during the end of the Pleistocene or the early Holocene on other Guadeloupe islands, in the same enigmatic way as on Marie-Galante Island. This possibility seems, nevertheless, difficult to explain considering the large size and high ecosystem diversity of the Guadeloupe islands and the survival of *Boa* on other nearby similar large islands, such as Dominica and Martinique, throughout the Holocene. The timing of the extinction of *Boa* in Guadeloupe is unlikely to reflect a paleontological bias considering the similar evidence for the Pleistocene extinction of this taxon in three distinct Marie-Galante deposits and the absence of this snake in both archeological and natural Holocene deposits from Marie-Galante and other Guadeloupe islands. The extinction of *Boa* is thus likely to be linked to a natural phenomenon. However, on account of the lack of data beyond Marie-Galante for the first half of the Holocene and the still elusive Amerindian preceramic populations (Siegel et al., 2015), the first human communities colonizing the Guadeloupe islands, we cannot rule out the role of human populations in some of these putative extinctions, as seems to have been the case on Antigua (Steadman et al., 1984; Pregill et al., 1994). The discovery of more fossil evidence of the past occurrence of *Boa* in the Guadeloupe islands is thus required to provide solid ground for its past occurrence and the timing and reasons of its extinction on all the Guadeloupe islands.

CONCLUSIONS

Our results lead to a better description and identification of the fossil, possibly dwarf, Marie-Galante *Boa*, described here as a new species, *Boa blanchardensis*. However, we encountered serious difficulties in proposing causes for its extinction in the light of the currently existing data concerning Marie-Galante fossil fauna. Our data confirm that the history of the Lesser Antillean *Boa* is complex and that an important radiation of these snakes probably occurred in this area in the past. However, in contrast to several other squamate taxa in Guadeloupe (Bochaton et al., 2016a, 2016b, 2017a, 2017b), and unlike other Lesser Antillean boas, anthropogenic issues may not have been the primary factor impacting Guadeloupe *Boa* snakes. The modern relictual distribution area of the *Boa* in the Lesser Antilles thus may not be exclusively related to the human impact on insular ecosystems. Data concerning the precise timing of *Boa* extinctions in the Lesser Antilles are, however, at present too scarce to discuss all the possible reasons underlying the disappearance of this snake on nearly all the islands of the insular chain. Much work is still required to improve our overall knowledge of past Lesser Antillean fauna and its interactions with human populations, because fossil data are still scarce or absent for several islands.

ACKNOWLEDGMENTS

The authors thank A. M. Albino and J. C. Rage as well as an anonymous reviewer for their numerous, useful comments and corrections, which allowed us to improve the quality of this paper. J. C. Rage passed away shortly after reviewing this paper and we would like to express our most sincere homage to this eminent paleoherpetologist. We are also grateful to the excavation directors who provided access to the fossil material: C. Stouvenot, S. Grouard, and A. Lenoble. We especially thank A. Lenoble and the Blanchard Cave excavation team members for collecting and sorting most of the material described in this study. We also thank B. Angin who collected comparative specimens from Dominica and the Ministry of Agriculture and Forestry of Dominica for the donation of these specimens. We are also grateful to J. Rosado and the Museum of Comparative Zoology for providing comparative specimens. We are grateful to M. Lemoine, who takes care of the histological preparations, and to V. de Buffrénil and A. Houssaye, who let us use their microscopes and provided help with the histological interpretations. We also thank I. Ineich, A. Tresset, and J. Lescure for useful insights and bibliographic suggestions regarding the manuscript. This study was partly funded by the CNRS BIVAAG project: 'Biodiversité Insulaire Vertébrée, floristique et malacologique Ancienne de l'Archipel de Guadeloupe,' with support from a European PO FEDER grant (2007-2013 n°2/2.4/-33456), the Guadeloupe Regional Council, the DEAL of Guadeloupe, and the DAC of Guadeloupe. C. B. is supported by a fellowship of the FYSSEN foundation.

ORCID

Corentin Bochaton http://orcid.org/0000-0003-4954-0019

LITERATURE CITED

Albino, A. M. 2011. Morfología vertebral de *Boa constrictor* (Serpentes: Boidae) y la validez del género mioceno *Pseudoepicrates* Auffenberg, 1923 (sic). Ameghiniana 48:53–62.

Albino, A. M. 2012. First snake record from the Sarmiento Formation at La Gran Hondonada (Chubut province, Argentina). Ameghiniana 49:230–235.

Albino, A. M., and A. A. Carlini. 2008. First record of *Boa constrictor* (Serpentes, Boidae) in the Quaternary of South America. Journal of Herpetology 42:82–88.

Andrews, R. M. 1982. Patterns of growth in reptiles; pp. 273–320 in C. Gans and F. H. Pough (eds.), Biology of the Reptilia. Academic Press, New York.

Angin, B. 2014. Bat predation by the Dominica Boa (*Boa nebulosa*). Caribbean Herpetology 51:1–2.

Anonyme de Carpentras, A. 1618. Relation d'un voyage infortuné fait aux Indes occidentales par le Capitaine Fleury avec la description de quelques Isles qu'on y rencontre, par l'un de ceux de la compagnie qui fit le voyage; pp. 328 in Un flibustier français dans la mer des Antilles 1618–1620, third edition. Petite bibliothèque Payot, Paris.

Anthony, J., and R. G. Serra. 1950. Anatomie de l'appareil de la morsure chez "*Eunectes murinus*" L. (Boidae). Revista Brasileira de Biologia 10:23–44.

Arendt, W. J., and D. Anthony. 1986. Bat predation by the St. Lucia boa (*Boa constrictor orophias*). Caribbean Journal of Science 22:219–220.

Auffenberg, W. 1963. The fossil snakes of Florida. Tulane Studies in Zoology 10(3):131–216.

Bailon, S., C. Bochaton, and A. Lenoble. 2015. New data on Pleistocene and Holocene herpetofauna of Marie-Galante (Blanchard Cave, Guadeloupe Islands, French West Indies): insular faunal turnover and human impact. Quaternary Science Reviews 128:127–137.

Boback, S. M. 2003. Body size evolution in snakes: evidence from island populations. Copeia 2003:81–94.

Boback, S. M. 2006. A morphometric comparison of island and mainland boas (*Boa constrictor*) in Belize. Copeia 2006:261–267.

Boback, S. M., C. Guyer, and J. Wiens. 2003. Empirical evidence for an optimal body size in snakes. Evolution 57:345–351.

Bochaton, C. 2016. Describing archaeological *Iguana* Laurenti, 1768 (Squamata: Iguanidae) populations: size and skeletal maturity. International Journal of Osteoarchaeology 26:716–724.

Bochaton, C., and M. E. Kemp. 2017. Reconstructing the body sizes of Quaternary lizards using *Pholidoscelis* Fitzinger, 1843 and *Anolis* Daudin, 1802 as case studies. Journal of Vertebrate Paleontology. doi: 10.1080/02724634.2017.1239626.

Bochaton, C., R. Boistel, and L. Charles. 2015a. X-ray microtomography provides first data about the feeding behavior of an endangered lizard, the Monstserrat galliwasp (*Diploglossus montisserrati*). Royal Society Open Science 2 (12):150461. doi:10.1098/rsos.150461.

Bochaton, C., R. Boistel, F. Cassagrande, S. Grouard, and S. Bailon. 2016a. A fossil *Diploglossus* (Squamata, Anguidae) lizard from Basse-Terre and Grande-Terre islands (Guadeloupe, French West-Indies). Scientific Reports 6:28475. doi: 10.1038/srep28475.

Bochaton, C., S. Bailon, I. Ineich, M. Breuil, A. Tresset, and S. Grouard. 2016b. From a thriving past to an uncertain future: zooarchaeological evidence of two millennia of human impact on a large emblematic lizard (*Iguana delicatissima*) on the Guadeloupe Islands (French West Indies). Quaternary Science Reviews 150:172–183.

Bochaton, C., R. Boistel, S. Grouard, I. Ineich, A. Tresset, and S. Bailon. 2017a. Evolution, diversity and interactions with past human populations of recently extinct *Pholidoscelis* lizards (Squamata: Teiidae) from the Guadeloupe Islands (French West-Indies). Historical Biology. doi: 10.1080/08912963.2017.1343824.

Bochaton, C., S. Grouard, R. Cornette, I. Ineich, A. Tresset, and S. Bailon. 2015b. Fossil and subfossil herpetofauna from Cadet 2 Cave (Marie-Galante, Guadeloupe Islands, F. W. I.): evolution of an insular herpetofauna since the Late Pleistocene. Comptes Rendus Palévol 14:101–110.

Bochaton, C., S. Bailon, A. Herrel, S. Grouard, I. Ineich, A. Tresset, and R. Cornette. 2017b. Human impacts reduce morphological diversity in an insular species of lizard. Proceedings of the Royal Society B: Biological Sciences 284:20170921.

Boudadi-Maligne, M., S. Bailon, C. Bochaton, F. Cassagrande, S. Grouard, N. Serrand, and A. Lenoble. 2016. Evidence for historical human-induced extinctions of vertebrate species on La Désirade (French West Indies). Quaternary Research 85:54–65.

Brace, S., S. T. Turvey, M. Weksler, M. L. P. Hoogland, and I. Barnes. 2015. Unexpected evolutionary diversity in a recently extinct Caribbean mammal radiation. Proceedings of the Royal Society B: Biological Sciences 282:20142371.

Breuil, M. 2009. The terrestrial herpetofauna of Martinique: past, present, future. Applied Herpetology 6:123–149.

Card, D. C., D. R. Schield, R. H. Adams, A. B. Corbin, B. W. Perry, A. L. Andrew, G. I. M. Pasquesi, E. N. Smith, T. Jezkova, S. M. Boback, W. Booth, and T. A. Castoe. 2016. Phylogeographic and population genetic analyses reveal multiple species of *Boa* and independent origins of insular dwarfism. Molecular Phylogenetics and Evolution 102:104–116.

Cundall, D., and F. Irish. 2008. The snake skull; pp. 349–362 in C. Gans, A. S. Gaunt, and K. Adler (eds.), The Skull of Lepidosauria, Biology of the Reptilia, Volume 20. Society for the Study of Amphibians and Reptiles, Ithaca, New York.

de Waal, M. S. 2006. Pre-Columbian social organization and interaction interpreted through the study of settlement patterns: an archaeological case-study of the pointe des Châteaux, La Désirade and les Îles de la Petite-Terre micro-region, Guadeloupe, F.W.I. Ph.D. dissertation, Leiden University, Leiden, The Netherlands, 419 pp.

Du Tertre, J.-B. 1654. Histoire générale des isles de S. Christophe, de la Guadeloupe, de la Martinique, et autres dans l'Amérique. Chez Jacques Langlois et Emmanuel Langlois, Paris, 542 pp.

Gala, M., and A. Lenoble. 2015. Evidence of the former existence of an endemic macaw in Guadeloupe, Lesser Antilles. Journal of Ornithology 156:1061–1066.

Graham Reynolds, R., M. L. Niemiller, and L. J. Revell. 2014. Toward a Tree-of-Life for the boas and pythons: multilocus species-level phylogeny with unprecedented taxon sampling. Molecular Phylogenetics and Evolution 71:201–213.

Gray, J. E. 1825. A synopsis of the genera of reptiles and Amphibia, with a description of some new species. Annals of Philosophy New Series 2:193–217.

Grouard, S. 2001. Subsistance, systèmes techniques et gestion territoriale en milieu insulaire antillais précolombien—exploitation des vertébrés et des crustacés aux époques Saladoïdes et Troumassoïdes de Guadeloupe (400 av. J.-C. à 1500 ap. J.-C.). Ph.D. dissertation, Université Paris X, Paris, 1073 pp.

Grouard, S. 2010. Caribbean archaeozoology; pp. 133–151 in G. Mengoni Goñalons, J. Arroyo-Cabrales, Ó. J. Polaco, and F. J. Aguilar (eds.), Estado actual de la Arqueozoología Latinoamericana [Current advances in Latin-American Archaeozoology]. International Council for Archaeozoology and Universidad de Buenos Aires, México.

Head, J. J., A. F. Rincon, C. Suarez, C. Montes, and C. Jaramillo. 2012. Fossil evidence for earliest Neogene American faunal interchange: *Boa* (Serpentes, Boinae) from the early Miocene of Panama. Journal of Vertebrate Paleontology 32:1328–1334.

Henderson, R., and R. Powell. 2009. Natural History of West Indian Reptiles and Amphibians. University Press of Florida, Gainesville, Florida, 496 pp.

Hoffstetter, R. 1939. Contribution à l'étude des elapidæ actuels et fossiles et de l'ostéologie des ophidiens. Archives du Muséum d'Historie Naturelle de Lyon 15:1–79.

Hoffstetter, R., and J. P. Gasc. 1969. Vertebrae and ribs of modern reptiles; pp. 201–310 in C. Gans (ed.), Biology of the Reptilia, Volume 1: Morphology. Academic Press, London.

Houssaye, A., R. Boistel, W. Böhme, and A. Herrel. 2013. Jack-of-all-trades master of all? Snake vertebrae have a generalist inner organization. Naturwissenschaften 100:997–1006.

Houssaye, A., A. Mazurier, A. Herrel, V. Volpato, P. Tafforeau, R. Boistel, and V. de Buffrénil. 2010. Vertebral microanatomy in squamates: structure, growth and ecological correlates. Journal of Anatomy 217:715–727.

Hsiou, A. S., and A. M. Albino. 2009. Presence of the genus *Eunectes* (Serpentes, Boidae) in the Neogene of Southwestern Amazonia, Brazil. Journal of Herpetology 43:612–619.

Kemp, M. E., and E. A. Hadly. 2015. Extinction biases in Quaternary Caribbean lizards. Global Ecology and Biogeography 24:1281–1289.

Keogh, J. S., I. A. W. Scott, and C. Hayes. 2005. Rapid and repeated origin of insular gigantism and dwarfism in Australian tiger snakes. Evolution 59:226–233.

Kluge, A. G. 1991. Boine snake phylogeny and research cycles. Miscellaneous Publications Museum of Zoology, University of Michigan 178:1–68.

Labat, J.-B. 1724. Nouveau Voyage aux Isles de l'Amerique, Volume 1. P. Husson, T. Johnson, P. Gosse, J. van Duren, R. Alberts and C. Le Vier, La Haye, 366p.

Linnaeus, C. 1758. Systema Naturae per Regna Tria Naturae, Secundum Classes, Ordines, Genera, Species, cum Characteribus, Differentiis, Synonymis, Locis. Tomus I. Editio decima, reformata. Laurentii Salvii, Stockholm, 824 pp.

Luiselli, L., F. Petrozzi, K. Mebert, M. A. L. Zuffi, and G. Amori. 2015. Resource partitioning and dwarfism patterns between sympatric snakes in a micro-insular Mediterranean environment. Ecological Research 30:527–535.

McDowell, S. B. 2008. The skull of Serpentes; pp. 467–738 in C. Gans, A. S. Gaunt, and K. Adler (eds.), The Skull and Appendicular Locomotor Apparatus of Lepidosauria, Biology of the Reptilia, Morphology I, Volume 21. Society for the Study of Amphibians and Reptiles, Ithaca, New York.

Moreau de Jonnès, A. 1816. Monographie du Trigonocéphale des Antilles, ou Grande Vipère Fer-de-Lance de La Martinique: Lue à l'Académie Royale des Sciences, dans sa Séance du 5 Août 1816. Imprimerie de Migneret, Paris, 42 pp.

Mosimann, J. E., and F. C. James. 1979. New statistical methods for allometry with application to Florida Red-Winged Blackbirds. Evolution 33:444–459.

Nopcsa, F. 1923. Die Familien der Reptilien. Verlag von Gebrüder Borntraeger, Berlin, 210 pp.

Onary-Alves, S. Y., A. S. Hsiou, and A. D. Rincón. 2016. The northernmost South American fossil record of *Boa constrictor* (Boidae, Boinae) from the Plio–Pleistocene of El Breal de Orocual (Venezuela). Alcheringa 41:1–8.

Oppel, M. 1811. Die Ordnungen, Familien und Gattungen der Reptilien als Prodrom einer Naturgeschichte derselben. Lindauer, Munich, 87 pp.

Paradis, E., S. Blomberg, B. Bolker, J. Claude, H. S. Cuong, R. Desper, G. Didier, B. Durand, J. Dutheil, O. Gascuel, C. Heibl, A. Ives, D. Lawson, V. Lefort, P. Legendre, J. Lemon, R. McCloskey, J. Nylander, R. Opgen-Rhein, A.-A. Popescu, M. Royer-Carenzi, K. Schliep, K. Strimmer, and D. de Vienne. 2015. Ape: analyses of phylogenetics and evolution. Available at ape-package.ird.fr. Accessed July 14, 2017.

Pedersen, S., H. Genoways, and P. Freeman. 1996. Notes on bats from Montserrat (Lesser Antilles) with comments concerning the effects of Hurricane Hugo. Mammalogy Papers of the University of Nebraska State Museum 32:206–213.

Powell, R., and R. W. Henderson. 2012. Island list of West Indian amphibians and reptiles. Bulletin of Florida Museum of Natural History 51:85–166.

Pregill, G. K., D. W. Steadman, and D. R. Watters. 1994. Late Quaternary vertebrate faunas of the Lesser Antilles: historical components of Caribbean biogeography. Bulletin of Carnegie Museum of Natural History 30:1–51.

Pregill, G. K., D. W. Steadman, S. L. Olson, and F. V. Grady. 1988. Late Holocene fossil vertebrates from Burma Quarry, Antigua, Lesser Antilles. Smithsonian Contributions to Zoology 463:1–27.

Rage, J. C. 2001. Fossil snakes from the Palaeocene of São Jose de Itaborai, Brazil. Part 2. Boidae. Palaeovertebrata 30:111–150.

Reagan, D. P. 1991. The response of *Anolis* lizards to hurricane-induced habitat changes in a Puerto Rican rain forest. Biotropica 23:468–474.

Rieppel, O. 1979. The evolution of the basicranium in the Henophidia (Reptilia: Serpentes). Zoological Journal of the Linnean Society 66:411–431.

Rieppel, O., and H. Zaher. 2001. The development of the skull in *Acrochordus granulatus* (Schneider) (Reptilia: Serpentes), with special consideration of the otico-occipital complex. Journal of Morphology 249:252–266.

Ripley, B., B. Venables, D. M. Bates, K. Hornick, A. Gebhardt, and D. Firth. 2016. MASS: support functions and datasets for Venables and Ripley's MASS. Available at www2.uaem.mx/r-mirror/web/packages/MASS/index.html. Accessed February 14, 2017.

Rochefort, C. D. 1658. Histoire Naturelle et Morale des Antilles de l'Amérique. Histoire Générale des Antilles Habitées par les Français. Arnould Liers, Rotterdam, 558 pp.

Royer, A., B. Malaizé, C. Lécuyer, A. Queffelec, K. Charlier, T. Caley, and A. Lenoble. 2017. A high-resolution temporal record of environmental changes in the Eastern Caribbean (Guadeloupe) from 40 to 10 ka BP. Quaternary Science Reviews 155:198–212.

Siegel, P. E., J. G. Jones, D. M. Pearsall, N. P. Dunning, P. Farrell, N. A. Duncan, J. H. Curtis, and S. K. Singh. 2015. Paleoenvironmental evidence for first human colonization of the eastern Caribbean. Quaternary Science Reviews 129:275–295.

Sierpe, V. 2011. Analyses, détermination et évaluation du complexe archéozoologique insulaire de l'abri Cadet 3, Marie-Galante, Archipel de la Guadeloupe. M.Sc. thesis, Muséum national d'Histoire naturelle, Paris, 116 pp.

Soto-Centeno, J. A., and D. W. Steadman. 2015. Fossils reject climate change as the cause of extinction of Caribbean bats. Scientific Reports 5:7971.

Steadman, D. W., G. K. Pregill, and S. L. Olson. 1984. Fossil vertebrates from Antigua, Lesser Antilles: evidence for late Holocene human-caused extinctions in the West Indies. Proceedings of the National Academy of Sciences of the United States of America 81:4448–4451.

Steadman, D. W., N. A. Albury, B. Kakuk, J. I. Mead, J. A. Soto-Centeno, H. M. Singleton, and J. Franklin. 2015. Vertebrate community on an ice-age Caribbean island. Proceedings of the National Academy of Sciences of the United States of America 112:E5963–E5971.

Stoetzel, E., A. Royer, D. Cochard, and A. Lenoble. 2016. Late Quaternary changes in bat palaeobiodiversity and palaeobiogeography under climatic and anthropogenic pressure: new insights from Marie-Galante, Lesser Antilles. Quaternary Science Reviews 143:150–174.

Stouvenot, C., S. Grouard, S. Bailon, D. Bonnissent, A. Lenoble, N. Serrand, and V. Sierpe. 2014. L'abri sous roche Cadet 3 (Marie-Galante): un gisement à accumulations de faune et à vestiges archéologiques; pp. 77–102 in B., Bérard, and C. Losier (eds.), Archéologie Caraïbe, Taboui 2, Sidestone Press, Leiden.

Szyndlar, Z. 1984. Fossil snakes from Poland. Acta Zoologica Cracoviensia 1:1–156.

Szyndlar, Z., and J. C. Rage. 2003. Non-erycine Booidea from the Oligocene and Miocene of Europe. Institute of Systematics and Evolution of Animals, Krakow, Poland, 109 pp.

Tanaka, K. 2011. Phenotypic plasticity of body size in an insular population of snake. Herpetologica 67:46–57.

Thomas, M. E. 1974. Bats as food source for *Boa constrictor*. Journal of Herpetology 8:188.

Underwood, G. 1964. An anguid lizard from the Leeward islands. Breviora 200:1–10.

Underwood, G. 1976. A systematic analysis of boid snakes; pages 151–175 in A. d'A. Bellairs and C. B. Cox (eds.), Morphology and Biology of Reptiles. Linnean Society Symposium Series 3. Academic Press, London.

Waide, R. B. 1991. Summary of the response of animal populations to hurricanes in the Caribbean. Biotropica 23:508–512.

Walker, L. R., D. J. Lodge, N. V. L. Brokaw, and R. B. Waide. 1991. An introduction to hurricanes in the Caribbean. Biotropica 23:313–316.

Submitted September 5, 2017; revisions received January 30, 2018;
accepted March 12, 2018.
Handling editor: Jason Head.